Inflammation Research (2020) 69:105–113
https://doi.org/10.1007/s00011-019-01297-x

Inflammation Research

ORIGINAL RESEARCH PAPER

Immunomodulatory activity of hyaluronidase is associated with metabolic adaptations during acute inflammation

Priscilla A. T. Pereira[1,2] · Claudia S. Bitencourt[1,3] · Mouzarllem B. Reis[1] · Fabiani G. Frantz[1] · Carlos A. Sorgi[1] · Camila O. S. Souza[1] · Célio L. Silva[4] · Luiz G. Gardinassi[1] · Lúcia H. Faccioli[1]

Received: 20 June 2019 / Revised: 10 October 2019 / Accepted: 31 October 2019 / Published online: 21 November 2019

Abstract

Objective and design Investigate survival outcomes, and immunological and metabolomic effects of hyaluronidase (Hz) treatment during mouse models of acute inflammation and sepsis.

Methods Survival of C57Bl/6 mice was monitored after lethal challenge with lipopolysaccharide (LPS) or cecal and ligation puncture (CLP)-induced sepsis and treated with Hz or saline. Mice were also challenged with LPS and treated with Hz for leukocyte counting, cytokine quantification and determination of metabolomic profiles in the peritoneal fluid.

Results Hz treatment improved survival outcomes after lethal challenge with LPS or CLP-induced sepsis. LPS challenge promoted acute neutrophil accumulation and production of interleukin-1β (IL-1β) and IL-6 in the peritoneum, whereas Hz treatment suppressed neutrophil infiltration and cytokine production. We further characterized the metabolomic alterations caused by LPS challenge, which predicted activity of metabolic pathways related to fatty acids and eicosanoids. Hz treatment had a profound effect over the metabolic response, reflected by reductions of the relative levels of fatty acids.

Conclusion Collectively, these data demonstrate that Hz treatment is associated with metabolic reprogramming of pathways that sustain the inflammatory response.

Keywords Hyaluronidase · Hyaluronic acid · Sepsis · Acute inflammation · Metabolomics

Introduction

Hyaluronidase (Hz) is a family of enzymes that catalyze hyaluronic acid (HA) degradation, a glycosaminoglycan that is a major component of the extracellular matrix [1]. Hz activity induces tissue permeability, a feature that has been clinically explored to facilitate the dispersion of fluids such as anesthetics [1, 2]. HA catabolism generates fragments of different molecular masses with functions during

Responsible Editor: Dr. John Di Battista.

Priscilla A. T. Pereira and Claudia S. Bitencourt contributed equally to this work.

Electronic supplementary material The online version of this article (https://doi.org/10.1007/s00011-019-01297-x) contains supplementary material, which is available to authorized users.

✉ Luiz G. Gardinassi
gustavogardinassi@usp.br

✉ Lúcia H. Faccioli
faccioli@fcfrp.usp.br

[1] Departamento de Análises Clínicas, Toxicológicas e Bromatológicas. Faculdade de Ciências Farmacêuticas de Ribeirão Preto, Universidade de São Paulo, Avenida Do Café, s/n, Ribeirão Preto, SP 14040-903, Brazil

[2] Departamento de Medicina, Faculdades de Dracena, Fundação Dracenense de Educação e Cultura, Rua Bahia, 332, Dracena, SP 17900-000, Brazil

[3] Centro Universitário das Faculdades Associadas Ao Ensino, Largo Engenheiro Paulo de A. Samdeville, 15, São João da Boa Vista, SP, Brazil

[4] Departamento de Bioquímica e Imunologia, Faculdade de Medicina de Ribeirão Preto, Universidade de São Paulo, Avenida Bandeirantes, 3900, Ribeirão Preto, SP 14049-900, Brazil

homeostasis and inflammation [3]. Indeed, HA fragments exhibit diverse immunomodulatory effects [4–6], while Hz treatment protects from bleomycin-induced lung injury [7, 8], accelerates wound healing [9] and suppresses inflammation in skin and colon [10]. Disruption of CD44 and HA interaction after Hz treatment has been implicated as an anti-inflammatory mechanism accounting for reduced neutrophil migration towards sites of lipopolysaccharide (LPS)-induced inflammation [11]. Other immunomodulatory effects of Hz treatment remain incompletely understood.

Upon infection, the inflammatory process is critical to clear pathogens, but deregulated host responses might culminate in clinical complications such as sepsis. This condition is characterized by an early acute hyperinflammatory state that causes tissue damage and may progress to multiple organ dysfunction and eventually death [12]. The inflammatory response is coupled with metabolic perturbations, which have been considered important features of sepsis pathogenesis [13, 14]. Metabolic adaptations are critical for proper activation and effector functions of immune cells during inflammation, while metabolic reprogramming at the tissue level impacts not only damage repair but also recovery of organ function [14]. Severity and prognosis of septic patients correlate with plasma levels of HA [15–17], while HA fragments exhibited protective properties in a rat model of sepsis [18]. These studies suggest that HA catabolism may play important functions during sepsis.

Here, we demonstrated that Hz treatment enhances animal survival after lethal challenge with LPS or CLP model of experimental sepsis. Hz suppressed the acute inflammatory response to LPS, reflected by reduced neutrophil accumulation and lower levels of pro-inflammatory cytokines in the peritoneal cavity. Metabolomics analyses of the peritoneal fluid indicate that LPS affected the activity of pathways involved with fatty acids, eicosanoids, vitamin E, bile acid and valine, leucine and isoleucine metabolism. Hz treatment of mice challenged with LPS affected activity of several metabolic pathways, including those related to fatty acids and eicosanoids. These data reveal that the immunomodulatory effects of Hz are associated with metabolic reprogramming of the inflammatory response.

Material and methods

Animals

Male, C57Bl6 mice (22–25 g) were obtained from the animal facilities of the Campus of Ribeirão Preto of the Universidade de São Paulo, Ribeirão Preto-SP, Brazil. Animals were maintained on a light/dark cycle with free access to food and water at animal facilities of the Faculdade de Medicina de Ribeirão Preto and Faculdade de Ciências Farmacêuticas de Ribeirão Preto, Universidade de São Paulo. All experiments were executed in accordance with the institutional guidelines for ethics in animal experimentation approved by the Animal Care Committee of the Universidade de São Paulo (Protocol No. 0142016-1).

Reagents

Commercial bovine testis-derived Hz Type IV-S was purchased from Sigma-Aldrich (St. Louis, MO, USA). Invanz antibiotic was from Merck Sharp & Dohme (Ertapenem, Whitehouse Station, NJ, USA). Lipopolysaccharide (LPS) of *Escherichia coli* 0111:B4 was from Sigma-Aldrich (St. Louis, MO, USA). ELISA antibodies to measure cytokines were from R&D Systems (Minneapolis, MN, USA). Diff-Quick staining was purchased from Laborclin (Paraná, Brazil). Endotoxin contamination of commercial bovine testis-derived Hz Type IV-S was verified with LAL test (QCL-1000, Bio Whittaker, Cambrex Company, USA).

Hz treatment and LPS challenge

Endotoxemia was induced in mice by intraperitoneal (i.p.) injection of LPS dissolved in 0.3 mL of phosphate-buffered saline (PBS) at the doses indicated in the Supplementary Fig. 1. Control groups received sterile PBS. Tree hours (h) after LPS injection, mice were treated with 16 U of Hz (dissolved in 0.3 mL of PBS) every 8 h. Survival was monitored for up to 14 days. There was minimal endotoxin contamination of Hz used in this study, with a mean concentration of 0.00002 EU/ml.

Cecal ligation and puncture (CLP)

CLP surgery was performed on mice as described previously [19]. Briefly, the cecum was punctured 12 times with a 21-gauge needle. Both sham surgery and CLP mice were treated with the antibiotic Invanz (Ertapenem, Merck Sharp & Dohme, Inc., Whitehouse Station, NJ, USA) administrated at 75 mg/kg via intraperitoneal beginning at 3 h after surgery and re-injected every 24 h until day 3 after surgery. Thirty minutes after antibiotic injection, Hz (16 U/mouse) was administered every 8 h and survival was monitored for 8 days.

Leukocyte counting in the peritoneal fluid

Mice were anesthetized with ketamine (100 mg/kg) (Dopaser®, Minas Gerais, Brazil) and xylazine (10 mg/kg) (Agener União, São Paulo, Brazil). Following euthanasia in CO_2 chamber, 3 mL of PBS was added into the abdominal cavity, which was gently massaged for 1 min. The peritoneal fluid was collected with a needle inserted into the inguinal

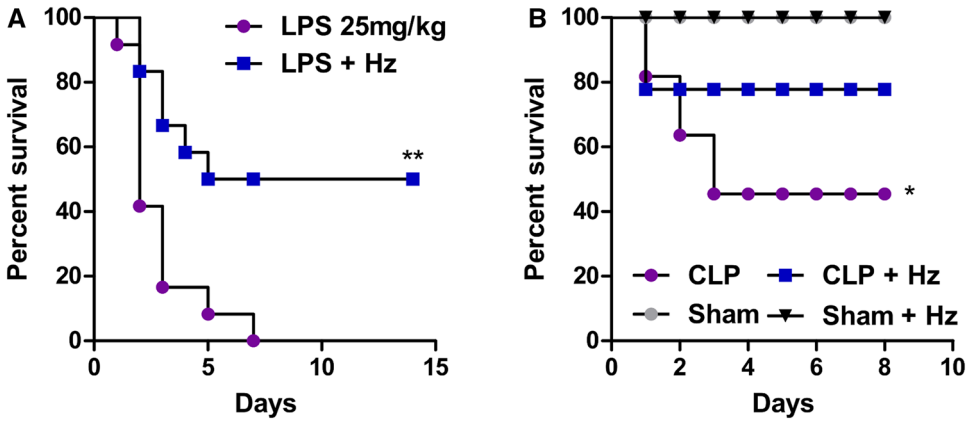

Fig. 1 Hyaluronidase (Hz) treatment improves outcomes of experimental models of sepsis. **a** C57Bl6 mice were injected with 25 mg/kg of LPS via i.p., and after 3 h they were treated with 16 U of Hz every 8 h and survival was monitored for 14 days. Data represent one independent experiment, using 12 animals per group ($n=12$). (**) $p=0.002$ using log-rank test. **b** C57Bl6 mice were subjected to cecal and ligation puncture (CLP) sepsis model or only submitted to surgery without CLP (sham). Both sham surgery and CLP mice were treated with Invanz (75 mg/kg i.p.) beginning at 3 h after surgery and re-injected every 24 h until day 3 after surgery. Thirty minutes after antibiotic injection, Hz (16 U/mouse) was administered every 8 h and survival was monitored for 8 days. Data represent one independent experiment, using ten animals per group ($n=12$). (*) $p=0.02$ using log-rank test

region. Total leukocytes were counted in Turk solution using Neubauer chambers. Differential leukocyte counts were performed using Diff-Quick -stained slides.

Cytokine quantification

Peritoneal fluid levels of IL-β and IL-6 were determined by ELISA according to manufacturer's instructions (R&D Systems, Minneapolis, MN, USA). Sensitivities were > 10 pg/mL.

Metabolomics analysis

Sample processing was performed as described [20]. Briefly, peritoneal fluid samples were spiked with stable isotope internal standards and metabolites were enriched with solid-phase extraction cartridges (Hypersep C18-500 mg, 3 mL, Thermo Scientific-Bellefonte, PA, USA) and methanol/water as solvents. After metabolite extraction, samples were transferred to autosampler vials for LC–MS analysis using TripleTOF5600+ Mass Spectrometer (Sciex-Foster, CA, USA) coupled to an Ultra-High-Performance Liquid Chromatography (UHPLC) system (Nexera X2, Shimadzu-Kyoto, HO, Japan). Reversed-phase chromatography was accomplished with a 100 × 4.6 mm, 2.7 µm Ascentis Express C18 column (Supelco—St. Louis, MO, USA). The gradient consisted of Phase A, H2O/ACN/acetic acid (69.98:30:0.02, v/v/v) at pH 5.8 (adjusted with NH4OH), and Phase B, an ACN/isopropanol (70:30, v/v). Gradient elution was carried out for 25 min at a flow rate of 0.6 mL/min. Gradient conditions were as follows: 0 to 2.0 min, 0% B; 2.0 to 5.0 min, 15% B; 5.0 to 8.0 min, 20% B; 8.0 to 11.0 min, 35% B; 11.0 to 15.0 min, 70% B; and 15.0 to 19 min, 100% B. At 19.0 min, the gradient returned to the initial condition of 0% B, and the column was re-equilibrated until 25.0 min. Mass spectral data were acquired with negative electrospray ionization and the full scan of mass-to-charge ratio (*m/z*) ranged from 100 to 1500. Proteowizard software [21] was used to convert wiff files into mzXML files. Peak peaking, noise filtering, retention time and *m/z* alignment, and feature quantification were performed with apLCMS [22]. Three parameters define a metabolite feature: mass-to-charge ratio (*m/z*), retention time and intensity values. Data were log2 transformed and only features detected in at least 80% of samples from one group (5439 *m/z* features) were used in further analysis. Missing values were imputed using half mean of the feature across all samples. The mummichog software (version 2) was used for metabolic pathway enrichment analysis (mass accuracy under 10 ppm) [23]. Metabolite annotation and reporting include five confirmation levels [24]. In addition to tentatively annotated metabolites with mummichog software, we also report putatively annotated compounds (level 3) matching to *m/z* at KEGG database as previously described [25, 26] (mass accuracy under 10 ppm—Supplementary Data 1). Untargeted metabolomics data used in this study were deposited at the public repository Metabolomics Workbench, under accession number ST001255.

Statistical analyses

Data were evaluated with GraphPad Prims v 5 and expressed as mean ± standard error. Longitudinal comparisons were evaluated with ANOVA followed by Bonferroni or Newman–Keuls multi-comparison tests. Categorical comparisons

were evaluated with Student's *t* test, and survival rates were evaluated with log-rank test. Values of $p < 0.05$ were considered significant. For LC–MS data, statistical analyses were carried out using the R Language and Environment for Statistical Computing (R) v3.4. Significant differences were evaluated with the package *limma* and false discovery rate was calculated using Benjamini–Hochberg method. Heat maps were obtained with the package *gplots* and Pearson distance method with ward linkage algorithm were used for hierarchical clustering with the package *amap*. Manhattan and bubble plots were obtained with the package *ggplot2*.

Results

Hyaluronidase enhances survival in experimental models of sepsis

HA fragments modulate immune cells properties, while Hz treatment affects cellular recruitment during inflammation [7, 27]. To determine whether Hz treatment is beneficial during models of acute inflammation with LPS or CLP sepsis, we first determined sub-lethal and lethal doses of LPS injected in C57Bl/6 mice via intraperitoneal (i.p.) route ($n = 5$/dose). We observed that 100% of mice survived after 15 mg/kg of LPS challenge but succumbed to all other LPS doses (Fig. S1). Following**,** mice received an injection of 25 mg/kg of LPS and after 3 h, animals were treated with 16 U of Hz every 8 h for 14 days ($n = 12$/group). We observed 100% mortality of animals that received LPS within 7 days after the challenge, whereas Hz treatment rescued 50% of animal survival until the 14th day after the challenge (Fig. 1a). Mice were then submitted to CLP sepsis and treated with Hz every 8 h throughout 8 days ($n = 12$/group). We observed that 50% of the animals survived 8 days after CLP, whereas Hz treatment limited mortality to 20% of animals (Fig. 1b).

Hyaluronidase suppresses acute inflammation induced by LPS challenge

To understand early effects of Hz treatment on cellular recruitment and activation, mice were injected with 15 mg/kg of LPS via i.p. and treated with 16 U of Hz every 8 h for 24 h ($n = 5$–6/group). The peritoneal fluid was collected to evaluate leukocyte counts and cytokine quantification. Total cell counts remained similar between mice challenged with LPS and controls, but Hz treatment after LPS challenge reduced the number of total leukocytes in the peritoneum (Fig. 2a). Compared to controls, mononuclear cell counts were reduced, while those of eosinophils increased after both LPS challenge or Hz treatment (Fig. 2b, c, respectively). LPS challenge induced a marked increase in neutrophil infiltration into the peritoneum that was significantly reduced after Hz treatment (Fig. 2d). Neutrophil infiltration into the peritoneal cavity after LPS challenge correlated with increased levels of the pro-inflammatory cytokines IL-1β and IL-6, whose production was significantly suppressed by Hz treatment (Fig. 2e, f, respectively).

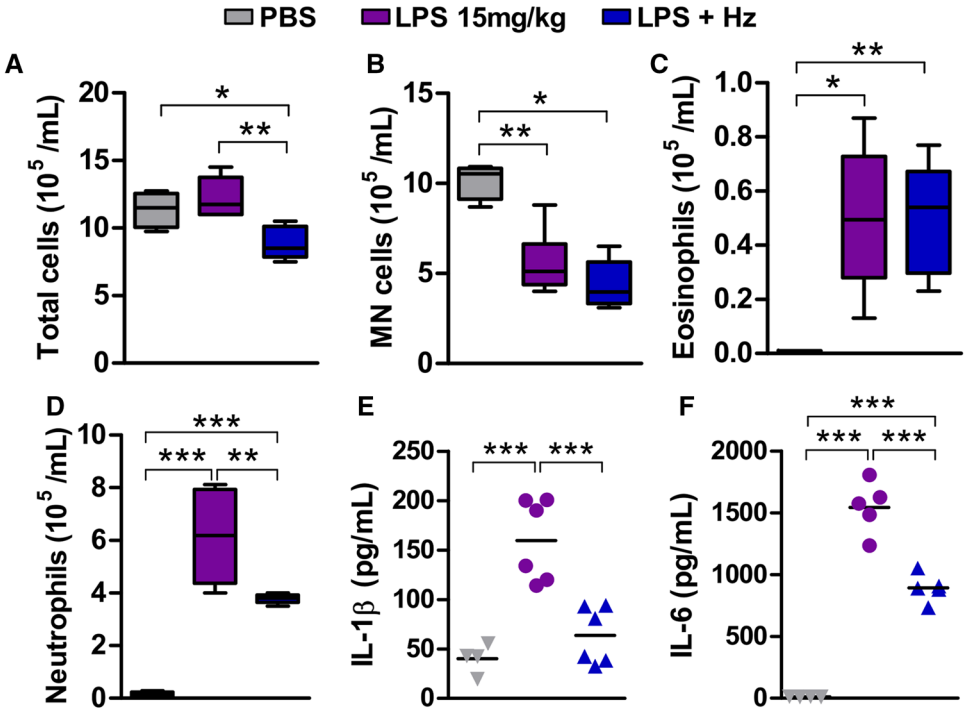

Fig. 2 Hyaluronidase (Hz) treatment suppresses LPS-induced acute inflammation. C57BL/6 mice were injected with 15 mg/kg of LPS via i.p., and after 3 h they were treated with 16 U of Hz every 8 h. Controls received sterile phosphate buffered saline (PBS). Peritoneal fluid was collected after 24 h of LPS challenge for estimation of **a** total cells, **b** mononuclear cells (MN), **c** eosinophil, and **d** polymorphonuclear cells counting; or quantification of **e** IL-1β and **f** IL-6. Data represent mean with min to max whiskers (**a**–**d**) or mean (**e**–**f**) of one out of two independent experiments, using five to six animals per group ($n = 5$–6). Significance is given by (*) $p < 0.05$ (**) $p < 0.01$ (***) $p < 0.001$

Metabolomic signatures of LPS-induced inflammation and Hz treatment

To obtain insights into the metabolic alterations promoted by Hz treatment during LPS-induced inflammation, mice were challenged with 15 mg/kg of LPS and treated with Hz every 8 h for 24 h ($n=6$/LPS for 3 h; $n=5$/LPS for 24 h; $n=6$/LPS + Hz for 24 h). PBS ($n=4$) and Hz alone ($n=5$) were injected as controls and the peritoneal fluid was collected for untargeted metabolomics analysis via high-resolution LC–MS. Data processing and filtering of missing values resulted in 5439 metabolite features used in further statistical and functional analysis (Supplementary Data 2). Compared to controls injected with PBS, the peritoneal fluid of mice challenged with LPS displayed increased the abundance of 400 metabolite features ($p<0.05$; 101 at FDR < 0.1) and reduced the abundance of 181 metabolite features in the peritoneal fluid after 3 h ($p<0.05$; 31 at FDR < 0.1; Fig. 3a and Supplementary Data 3). After 24 h, LPS challenge induced the differential abundance of 818 metabolite features ($p<0.05$; 323 at FDR < 0.05). Hz injection alone affected the abundance of 896 metabolite features ($p<0.05$; 409 at FDR < 0.05). Strikingly, the peritoneal fluid of mice challenged with LPS and treated with Hz displayed increased abundance of 228 ($p<0.05$; 79 at FDR < 0.1) and reduced abundance of 551 metabolite features ($p<0.05$; 152 at FDR < 0.1; Fig. 3a and Supplementary Data 3). Further analysis demonstrated large overlap among metabolite features modulated by LPS or Hz treatment alone, with 237 common features affected by LPS at 3 and 24 h and Hz for 24 h (Fig. 3b). We also observed metabolite features whose levels were specifically affected by LPS, Hz alone or LPS + Hz when compared to PBS control. The peritoneal fluid from mice challenged with LPS and treated with Hz exhibited the largest number of specifically modulated features (Fig. 3b).

To determine the metabolomic signatures induced by LPS challenge throughout 24 h, we conducted analysis of variance (ANOVA) using data from mice injected with PBS or LPS at 3 or 24 h after challenge. LPS modulated the abundance of 737 metabolite features ($p<0.05$; 193 at FDR < 0.05; Fig. 4a). Hierarchical clustering of significant features revealed that most of them accumulated over time, while a small cluster of features displayed higher abundance only after 24 h (Fig. 4b). We used the *mummichog* software [23] to predict metabolic pathways enriched by these significant features. The analysis suggests that significant features were mainly involved in fatty acid and eicosanoid metabolism, which enriched in pathways such as arachidonic acid metabolism, fatty acid activation, linoleate metabolism, de novo fatty acid biosynthesis and prostaglandin formation (Fig. 4c). Alterations in fatty acid pathways are represented by dynamic abundance of oleic acid, linoleic acid and linolenic acid (Fig. 4f).

To understand the effects of Hz treatment over LPS challenge, we first subtracted the mean log2 intensity values of metabolite features measured for PBS controls to control for potential confounding factors. Following, we conducted

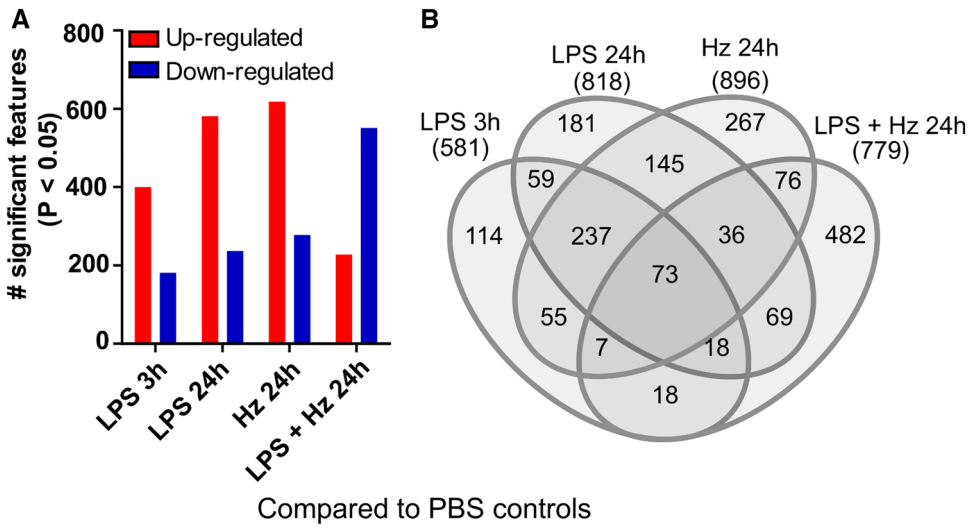

Fig. 3 Metabolomics analysis of peritoneal fluid during LPS challenge and Hz treatment compared to PBS controls. C57BL/6 mice were injected with 15 mg/kg of LPS via i.p., and after 3 h they were treated with 16 U of Hz every 8 h. Controls received sterile phosphate buffered saline (PBS; $n=4$). Peritoneal fluid was collected after 3 ($n=6$) or 24 h ($n=5$) of LPS challenge, 24 h after Hz injection ($n=5$) or 24 h after LPS challenge and Hz treatment ($n=6$) for LC–MS analysis. **a** Differential abundance of metabolite features compared to mice that received PBS. Significant metabolite features ($p<0.05$) were identified with moderated *t* test using *limma* package for R. **b** Venn diagram comparing overlapping and non-overlapping differentially abundant metabolite features compared to PBS controls

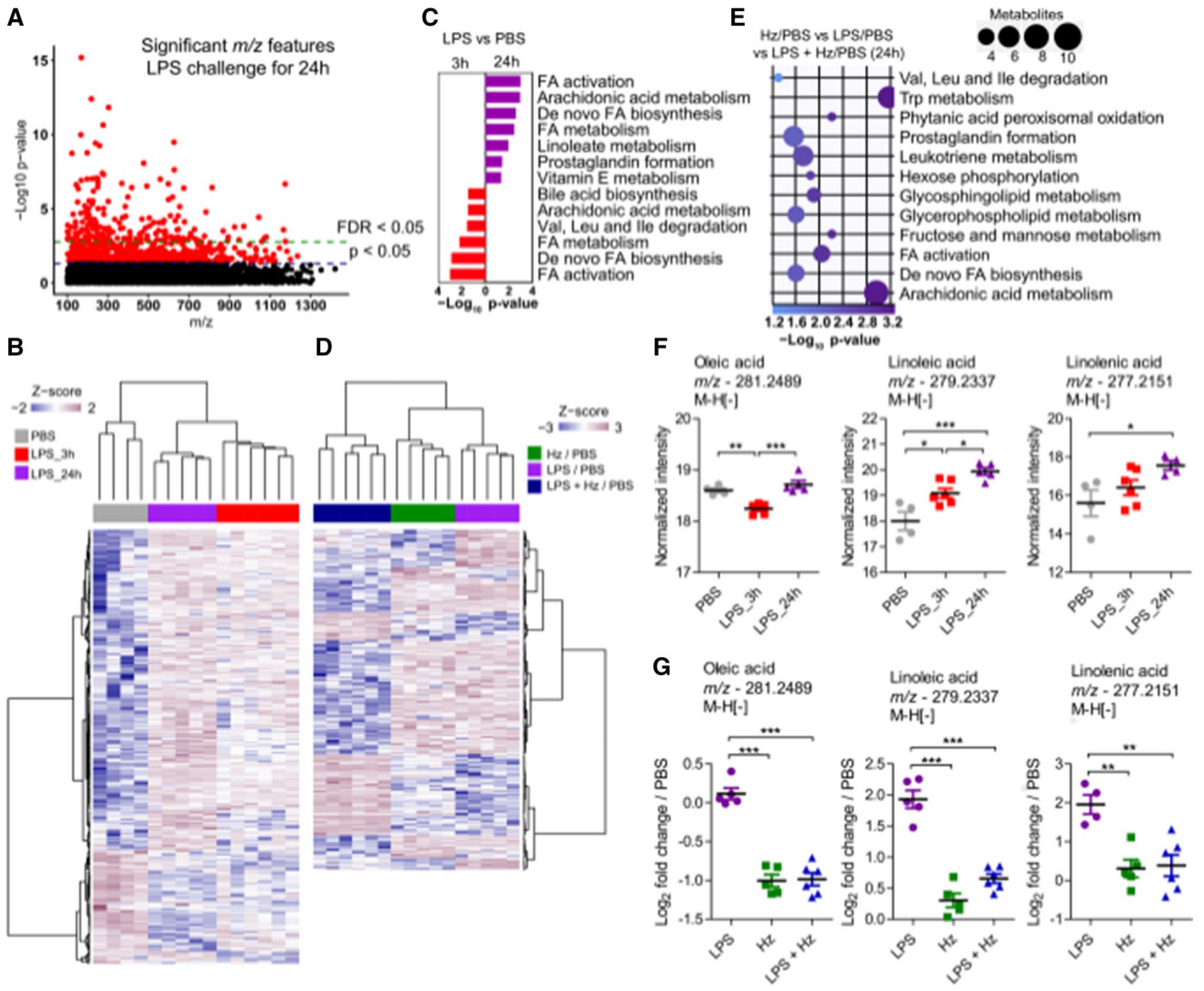

Fig. 4 Metabolomic signatures of LPS challenge, Hz injection and Hz treatment after LPS challenge. C57BL/6 mice were injected with 15 mg/kg of LPS via i.p., and after 3 h they were treated with 16 U of Hz every 8 h. Controls received 16 U of Hz every 8 h or sterile phosphate buffered saline (PBS). Peritoneal fluid was collected after 24 h of LPS challenge and/or Hz treatment for LC–MS analysis. These analyses were performed with the same samples described in Fig. 3 ($n = 4$–6 mice/group). **a** Manhattan plot for significant metabolite features throughout 24 h of LPS challenge identified with ANOVA ($p < 0.05$ or FDR < 0.05). **b** Hierarchical clustering based on differentially abundant metabolite features (ANOVA—FDR < 0.1) between PBS controls, LPS at 3 h or LPS at 24 h. **c** *Mummichog* analysis and metabolic pathway enrichment of differentially abundant metabolite features ($p < 0.05$) throughout 24 h of LPS challenge compared to PBS controls. Only pathways enriched by at least 4 metabolites and significance of $p < 0.05$ are shown. **d** Hierarchical clustering based on differentially abundant metabolite features (ANOVA—FDR < 0.1) using control (PBS) subtracted intensity values ($\log_2$ fold change related to PBS) from LPS, Hz or LPS + Hz at 24 h after the challenge. **c** *Mummichog* analysis and metabolic pathway enrichment of differentially abundant metabolite features ($p < 0.05$) between PBS subtracted intensity values ($\log_2$ fold change related to PBS) from LPS, Hz or LPS + Hz at 24 h after the challenge. Only pathways enriched by at least 4 metabolites and significance of $p < 0.05$ are shown. **f**–**g** Distribution of predicted metabolites differing between LPS vs PBS throughout 24 h of LPS challenge (**f**) or between LPS /PBS, Hz / PBS and LPS + Hz / PBS (**g**). The metabolite labels are based on tentative annotation from the *mummichog* software. Mean values, standard error (SE) and significance levels are shown (*) $p < 0.05$ (**) $p < 0.01$ (***) $p < 0.001$

ANOVA using data from mice challenged with LPS or injected with Hz alone or mice challenged with LPS and treated with Hz at 24 h after the challenge. Hierarchical clustering of differentially abundant metabolite features demonstrates highly distinct metabolomic profiles for each group (Fig. 4d). *Mummichog* analysis predicted altered activity of pathways involved with fatty acids, eicosanoids, carbohydrates, glycerophospholipids, glycosphingolipids and amino acids, from which tryptophan metabolism was the most significant (Fig. 4e). Compared to PBS treatment,

levels of oleic acid returned to baseline after 24 h of LPS stimulation (Fig. 4f). However, levels of this fatty acid were significantly reduced by treatments with Hz alone or LPS + Hz, suggesting an effect that is independent of LPS stimulation (Fig. 4g). On the other hand, treatment with Hz alone did not impact levels of linoleic and linolenic acids, whose levels were similar to that of controls (PBS). While levels of both linoleic and linolenic acids continued to rise after 24 h of LPS stimulation (Fig. 4f), Hz treatment after LPS challenge had a striking impact on the relative levels of these fatty acids (Fig. 4g).

Discussion

In this study, we demonstrated that early after LPS challenge, Hz treatment has a profound impact on neutrophil recruitment and cytokine production that are coupled with dynamic metabolic adaptations in the peritoneum. Importantly, we showed that Hz treatment improved outcomes of lethal challenge with LPS or CLP-induced sepsis. Although these data provide insights about the effects of Hz treatment during systemic inflammatory conditions, further investigation is necessary to delineate whether Hz activity and HA fragments actively induce metabolic reprogramming, or whether the reported molecular signatures only reflect metabolic phenotypes after inflammation has been suppressed.

Leukocytes express HA-binding receptors such as CD44 and receptor for HA mediated motility (RHAMM/CD168), whose signaling promotes cell migration and proliferation [28]. These cellular processes are coupled with metabolic adaptations that maintain energetic needs and promote regulatory activities. Hz treatment was associated with altered activity of pathways that are critical for the inflammatory response. LPS stimulation of innate immune cells, such as macrophages, increases the energetic and biosynthetic demands. To achieve this, they increase the glycolytic activity in detriment of oxidative phosphorylation [29]. Toll-like receptor (TLR) signaling enhances glycolysis in dendritic cells to expand fatty acid synthesis, which are used as building blocks of endoplasmic reticulum and Golgi to support production and secretion of inflammatory mediators [30]. Indeed, fatty acid metabolism is emerging as a critical regulator of the immune response [31]. Therefore, the accumulation of fatty acids in the peritoneal cavity of mice challenged with LPS is likely the result of increased fatty acid biosynthesis coupled with reduced fatty acid oxidation after cellular activation by TLR signaling. The immunomodulatory effects of Hz treatment correlated with reduced levels of fatty acids, suggesting that HA fragments interfere with energetic metabolism during immune cell activation. Recent study demonstrated that HA accumulates in sites of reactive adipogenesis, a local expansion of preadipocytes following inflammation caused by dextran sodium sulfate in the colon or skin infection with *Staphylococcus aureus* in mice [10]. In line with our findings, Hz treatment inhibited reactive adipogenesis, which correlated with reduced inflammatory cell infiltration and production of IL-6 after *S. aureus* infection [10]. Hz treatment of mice challenged with LPS reduced lipid content in the peritoneum and could also reflect reduced reactive adipogenesis.

Metabolic pathway analysis predicted activity of eicosanoid metabolism, which is not surprising since this network of bioactive lipids is activated after LPS challenge in vitro and in vivo [32, 33]. Biosynthesis of arachidonic acid (AA) occurs via metabolism of linoleic and γ-linolenic acids, both of which accumulated in the peritoneum throughout LPS challenge and were reduced by Hz treatment. AA oxidation by distinct enzymes generates different products with non-redundant functions [34]. Leukotriene B_4 (LTB_4) mediates neutrophil migration into peritoneal cavity of mice submitted to CLP sepsis model [35]. Our data suggest that Hz treatment downregulates the availability or even biosynthesis of fatty acids, which could limit the production of inflammatory lipids. This is in accordance with reduced neutrophil recruitment into peritoneal cavity after Hz treatment of mice challenged with LPS. In addition, inhibition of cyclooxygenase 2 (COX-2) and synthesis of prostaglandin E_2 (PGE_2) improves early survival of mice challenged with LPS [36], while this lipid mediator boosts IL-1β production by macrophages [33, 37, 38]. Therefore, reduction of inflammatory lipids by Hz treatment could also account for reduced IL-1β production and must also influence neutrophil infiltration in the peritoneum after endotoxemia.

Neutrophil infiltration in the lung after CLP sepsis depends on CD44, but not on the interaction with HA, because Hz treatment had no effect on cellular recruitment and lung damage [39]. However, neutrophil infiltration into mouse air pouches challenged with LPS depends on the interaction between CD44 and HA [11], while endotoxemia induces neutrophil entrapment in the liver via interaction between CD44 expressed by neutrophils and HA composing tissues [40]. Blocking this interaction with Hz treatment reduced neutrophil adhesion in inflamed liver sinusoids [40] or infiltration into air pouches [11, 27]. Therefore, it is possible that Hz disrupted this interaction via HA degradation to reduce neutrophil infiltration in the peritoneal cavity during LPS-induced inflammation.

Of note, Hz injection alone induced metabolomic alterations that were quantitatively similar to that induced by LPS challenge when compared to PBS controls. Diverse studies have implicated HA fragments as danger-associated molecular patterns (DAMPS), which are recognized by TLR 2 and 4 and promote inflammatory responses [41]. However, there is also evidence for LPS contamination as the major driver of inflammation in mice injected with bovine testis-derived

hyaluronidase IV-S (endotoxin contamination at 234 EU/mL) [11]. Prior exposure to endotoxin causes innate immune cells to become tolerant or refractory to a subsequent challenge with LPS [42]. Together, these findings may suggest that in our models, contaminating endotoxin, and not the enzyme Hz per se, is responsible for modulating the inflammatory response and control of mortality after lethal LPS challenge or CLP sepsis. Nevertheless, we observed minimal endotoxin contamination of the commercial bovine testis-derived Hz Type IV-S used in this study (0.00002 EU/mL). Moreover, to induce endotoxin tolerance, mice or cells in vitro are previously exposed to small doses of LPS before subsequent challenge with higher doses of LPS [43]. This operational mechanism leads to the epigenetic reprogramming of macrophages, which reduces the production of some pro-inflammatory mediators, such as TNF-α. For the experiments conducted in this study, mice were challenged with single dose of LPS at 15 mg/Kg, while the endotoxin contamination of Hz preparations would never reach such higher concentrations. Therefore, molecular reprogramming of innate immune cells by contaminating endotoxin is unlikely to drive the metabolic adaptations after Hz treatment reported here. In addition, we included appropriate controls for metabolomics analysis (PBS and Hz alone), which were critical to eliminate potential confounding factors in the statistical analyses and to distinguish between effects caused by Hz alone and those occurring only after LPS challenge. Collectively, these data indicate that Hz promotes immuno-metabolic adaptations that are associated with improved survival outcomes during mouse models of systemic inflammation.

Acknowledgments This study was supported by the Fundação de Amparo à Pesquisa do Estado de São Paulo (FAPESP grant #2009/07169-5, #2014/07125-6 and EMU #2015/00658-1 to LF; FAPESP scholarship #2007/04741-4 to CB); the Conselho Nacional de Desenvolvimento Científico e Tecnológico (CNPq grant #302514/2015-5); and Coordenação de Aperfeiçoamento de Pessoal de Nível Superior Brasil (CAPES)–Código de Financiamento 001 (process #1746212, #88882.317663/2019-01 and #88887.363659/2019-00 to LG; #150991/2011-8 to CB).

Compliance with ethical standards

Conflict of interest The authors declare that they have no competing interests.

References

1. Buhren BA, Schrumpf H, Hoff N-P, Bölke E, Hilton S, Gerber PA. Hyaluronidase: from clinical applications to molecular and cellular mechanisms. Eur J Med Res. 2016;21:5.
2. Dunn AL, Heavner JE, Racz G, Day M. Hyaluronidase: a review of approved formulations, indications and off-label use in chronic pain management. Expert Opin Biol Ther. 2010;10:127–31.
3. Lee-Sayer SSM, Dong Y, Arif AA, Olsson M, Brown KL, Johnson P. The where, when, how, and why of hyaluronan binding by immune cells. Front Immunol. 2015;6:150.
4. Hodge-Dufour J, Noble PW, Horton MR, Bao C, Wysoka M, Burdick MD, et al. Induction of IL-12 and chemokines by hyaluronan requires adhesion-dependent priming of resident but not elicited macrophages. J Immunol. 1997;159:2492–500.
5. Horton MR, Burdick MD, Strieter RM, Bao C, Noble PW. Regulation of hyaluronan-induced chemokine gene expression by IL-10 and IFN-gamma in mouse macrophages. J Immunol. 1998;160:3023–30.
6. McKee CM, Penno MB, Cowman M, Burdick MD, Strieter RM, Bao C, et al. Hyaluronan (HA) fragments induce chemokine gene expression in alveolar macrophages. The role of HA size and CD44. J Clin Invest. 1996;98:2403–13.
7. Bitencourt CS, Pereira PA, Ramos SG, Sampaio SV, Arantes EC, Aronoff DM, et al. Hyaluronidase recruits mesenchymal-like cells to the lung and ameliorates fibrosis. Fibrogenesis Tissue Repair. 2011;4:3.
8. da Silva BC, Gelfuso GM, Pereira PAT, de Assis PA, Tefé-Silva C, Ramos SG, et al. Hyaluronidase-loaded PLGA Microparticles as a new strategy for the treatment of pulmonary fibrosis. Tissue Eng Part A. 2014;21:246–56.
9. Fronza M, Caetano GF, Leite MN, Bitencourt CS, Paula-Silva FWG, Andrade TAM, et al. Hyaluronidase modulates inflammatory response and accelerates the cutaneous wound healing. PLoS ONE. 2014;9:e112297.
10. Dokoshi T, Zhang L-J, Nakatsuji T, Adase CA, Sanford JA, Paladini RD, et al. Hyaluronidase inhibits reactive adipogenesis and inflammation of colon and skin. JCI Insight. 2018;3(21):e123072.
11. Huang Z, Zhao C, Chen Y, Cowell JA, Wei G, Kultti A, et al. Recombinant human hyaluronidase PH20 does not stimulate an acute inflammatory response and inhibits lipopolysaccharide-induced neutrophil recruitment in the air pouch model of inflammation. J Immunol. 2014;192:5285–95.
12. Martin GS. Sepsis, severe sepsis and septic shock: changes in incidence, pathogens and outcomes. Expert Rev Anti Infect Ther. 2012;10:701–6.
13. Angus DC, van der Poll T. Severe sepsis and septic shock. N Engl J Med. 2013;369:840–51.
14. Weis S, Carlos AR, Moita MR, Singh S, Blankenhaus B, Cardoso S, et al. Metabolic adaptation establishes disease tolerance to sepsis. Cell. 2017;169(1263–1275):e14.
15. Berg S. Hyaluronan turnover in relation to infection and sepsis. J Intern Med. 1997;242:73–7.
16. Yagmur E, Koch A, Haumann M, Kramann R, Trautwein C, Tacke F. Hyaluronan serum concentrations are elevated in critically ill patients and associated with disease severity. Clin Biochem. 2012;45:82–7.
17. Berg S, Brodin B, Hesselvik F, Laurent TC, Maller R. Elevated levels of plasma hyaluronan in septicaemia. Scand J Clin Lab Invest. 1988;48:727–32.
18. Liu Y-Y, Lee C-H, Dedaj R, Zhao H, Mrabat H, Sheidlin A, et al. High-molecular-weight hyaluronan—a possible new treatment for sepsis-induced lung injury: a preclinical study in mechanically ventilated rats. Crit Care. 2008;12:R102.
19. Wen H, Hogaboam CM, Gauldie J, Kunkel SL. Severe sepsis exacerbates cell-mediated immunity in the lung due to an altered dendritic cell cytokine profile. Am J Pathol. 2006;168:1940–50.
20. Sorgi CA, Peti APF, Petta T, Meirelles AFG, Fontanari C, de Moraes LAB, et al. Comprehensive high-resolution multiple-reaction monitoring mass spectrometry for targeted eicosanoid assays. Sci Data. 2018;5:180167.
21. Chambers MC, Maclean B, Burke R, Amodei D, Ruderman DL, Neumann S, et al. A cross-platform toolkit for mass spectrometry and proteomics. Nat Biotechnol. 2012;30:918–20.

22. Yu T, Park Y, Johnson JM, Jones DP. apLCMS—adaptive processing of high-resolution LC/MS data. Bioinformatics. 2009;25:1930–6.
23. Li S, Park Y, Duraisingham S, Strobel FH, Khan N, Soltow QA, et al. Predicting network activity from high throughput metabolomics. PLoS Comput Biol. 2013;9:e1003123.
24. Salek RM, Steinbeck C, Viant MR, Goodacre R, Dunn WB. The role of reporting standards for metabolite annotation and identification in metabolomic studies. Gigascience. 2013;2:13.
25. Gardinassi LG, Arévalo-Herrera M, Herrera S, Cordy RJ, Tran V, Smith MR, et al. Integrative metabolomics and transcriptomics signatures of clinical tolerance to Plasmodium vivax reveal activation of innate cell immunity and T cell signaling. Redox Biol. 2018;17:158–70.
26. Gardinassi LG, Cordy RJ, Lacerda MVG, Salinas JL, Monteiro WM, Melo GC, et al. Metabolome-wide association study of peripheral parasitemia in *Plasmodium vivax* malaria. Int J Med Microbiol. 2017;307:533–41.
27. Fronza M, Muhr C, da Silveira DSC, Sorgi CA, Rodrigues SF de P, Farsky SHP, et al. Hyaluronidase decreases neutrophils infiltration to the inflammatory site. Inflamm Res. 2016;65:533–42.
28. Nedvetzki S, Gonen E, Assayag N, Reich R, Williams RO, Thurmond RL, et al. RHAMM, a receptor for hyaluronan-mediated motility, compensates for CD44 in inflamed CD44-knockout mice: a different interpretation of redundancy. Proc Natl Acad Sci USA. 2004;101:18081–6.
29. Carroll RG, Zasłona Z, Galván-Peña S, Koppe EL, Sévin DC, Angiari S, et al. An unexpected link between fatty acid synthase and cholesterol synthesis in proinflammatory macrophage activation. J Biol Chem. 2018;293:5509–21.
30. Everts B, Amiel E, Huang SC-C, Smith AM, Chang C-H, Lam WY, et al. TLR-driven early glycolytic reprogramming via the kinases TBK1-IKKε supports the anabolic demands of dendritic cell activation. Nat Immunol. 2014;15:323–32.
31. Sinclair C, Bommakanti G, Gardinassi L, Loebbermann J, Johnson MJ, Hakimpour P, et al. mTOR regulates metabolic adaptation of APCs in the lung and controls the outcome of allergic inflammation. Science. 2017;357:1014–21.
32. Pacheco P, Bozza FA, Gomes RN, Bozza M, Weller PF, Castro-Faria-Neto HC, et al. Lipopolysaccharide-induced leukocyte lipid body formation in vivo: innate immunity elicited intracellular loci involved in eicosanoid metabolism. J Immunol. 2002;169:6498–506.
33. Zoccal KF, Gardinassi LG, Sorgi CA, Meirelles AFG, Bordon KCF, Glezer I, et al. CD36 shunts eicosanoid metabolism to repress CD14 licensed interleukin-1β release and inflammation. Front Immunol. 2018;9:890.
34. Dennis EA, Norris PC. Eicosanoid storm in infection and inflammation. Nat Rev Immunol. 2015;15:511–23.
35. Rios-Santos F, Benjamim CF, Zavery D, Ferreira SH, Cunha F de Q. A critical role of leukotriene B4 in neutrophil migration to infectious focus in cecal ligaton and puncture sepsis. Shock. 2003;19:61–5.
36. Reddy RC, Chen GH, Tateda K, Tsai WC, Phare SM, Mancuso P, et al. Selective inhibition of COX-2 improves early survival in murine endotoxemia but not in bacterial peritonitis. Am J Physiol Lung Cell Mol Physiol. 2001;281:L537–543.
37. Zoccal KF, Ferreira GZ, Prado MKB, Gardinassi LG, Sampaio SV, Faccioli LH. LTB4 and PGE2 modulate the release of MIP-1α and IL-1β by cells stimulated with Bothrops snake venoms. Toxicon. 2018;150:289–96.
38. Pereira PAT, Assis PA, Prado MKB, Ramos SG, Aronoff DM, de Paula-Silva FWG, et al. Prostaglandins D2and E2have opposite effects on alveolar macrophages infected with *Histoplasma capsulatum*. J Lipid Res. 2018;59:195–206.
39. Hasan Z, Palani K, Rahman M, Thorlacius H. Targeting CD44 expressed on neutrophils inhibits lung damage in abdominal sepsis. Shock. 2011;35:567–72.
40. McDonald B, McAvoy EF, Lam F, Gill V, de la Motte C, Savani RC, et al. Interaction of CD44 and hyaluronan is the dominant mechanism for neutrophil sequestration in inflamed liver sinusoids. J Exp Med. 2008;205:915–27.
41. Petrey AC, de la Motte CA. Hyaluronan, a Crucial regulator of inflammation. Front Immunol. 2014. https://www.ncbi.nlm.nih.gov/pmc/articles/PMC3949149/. Accessed 18 June 2019
42. Biswas SK, Lopez-Collazo E. Endotoxin tolerance: new mechanisms, molecules and clinical significance. Trends Immunol. 2009;30:475–87.
43. Melo ES, Barbeiro HV, Ariga S, Goloubkova T, Curi R, Velasco IT, et al. Immune cells and oxidative stress in the endotoxin tolerance mouse model. Braz J Med Biol Res. 2010;43:57–67.